Full Length Research Paper

Analysis of combined anti-tuberculous drug induced neurotoxicity in the cerebral cortex of adult wistar rats by immunohistochemistry

Fakoya Francis Adelade[1,2]*, Osoniyi Omolaja[3] and Obuotor Efere Martins[3]

[1]Department of Anatomy and Cell Biology, Faculty of Basic Medical Sciences, Obafemi Awolowo University, Ile-Ife, Nigeria.
[2]Department of Anatomical Sciences, St. George's University School of Medicine, True Blue, St. George's Grenada, The Caribbean.
[3]Department of Biochemistry, Faculty of Science, Obafemi Awolowo University, Ile-Ife, Nigeria

Combined Isoniazid (INH) and Rifampicin administration still remain as two of the main drugs of choice in the treatment regimes of tuberculosis (TB) world wide, particularly in Africa, where tuberculosis incidence rates are among the highest in the world. This study evaluated the effects of chronic administration of combined Isoniazid/Rifampicin on the cerebral cortex of the adult rats by immunohistochemistry. Adult wistar rats (average weight of 220 g) maintained under standard laboratory conditions were randomly grouped into treatment and control (n = 10). The treatment group A received combined INH + Rifampicin (50 mg/kg each, i.p) while the control group B received normal saline (0.5 ml, i.p.) only; daily at 1600 h for 15 days. Animals were sacrificed by cervical dislocation for whole brain weight determination (n = 6) and by whole body perfusion following anaesthesia for neurohistology and immunohistochemistry (n = 4) from each group. Coronal samples of the frontoparietal cortex were taken from each hemisphere and processed routinely for paraffin embedding followed by Nissl staining of 6 µm thick sections. 30 µm thick sections were cryo-sectioned at -23°C, after cryoprotection in 30% sucrose/phosphate buffered saline (PBS) from the remaining samples and reacted for flourescent glial fibrillary acidic protein (GFAP) immunoreactivity and terminal deoxynucleotidyl transferase dUTP nick end labeling (TUNEL) method for the detection of apoptosis. The treatment group showed highly reactive intracortical and subpial GFAP positive astrocytes, mostly localized as clusters, compared to the control; GFAP immunostaining intensity was quantified using Adobe Photoshop Element 6.0. Cerebral cortical lamina was well preserved in both groups, while neuronal pyknotism were not observed in the treatment group, compared to the controls. The treatment group showed intense darkly stained discrete cells, positive for the TUNEL signals. These microanatomical and microchemical changes suggest neurotoxicity of these drugs, which though was not overt clinically.

Key words: Tuberculosis, anti-tuberculous drugs, neurotoxicity, quantitative immunocytochemistry, adobe photoshop elements, astrogliosis, apoptosis, cerebral cortex, isoniazid, rifampicin.

INTRODUCTION

The global burden of disease caused by tuberculosis (TB) was estimated in 2011 to be at 8.7 million incidence

*Corresponding author. E-mail: ffakoya@sgu.edu. Tel: +1(473)5349960. Fax: +1(473)4441602.

cases and 12 million prevalent cases (WHO, 2012). TB, a disease of poverty, is contagious and air borne, affecting mostly young adults in their productive years and ranks as the second leading cause of death from an infectious disease worldwide, after the human immunodeficiency virus (HIV). With a reported estimate of 8.7 million new cases of TB (13% co-infected with HIV), 1.4 million people die from TB, including almost one million deaths among HIV-negative individuals and 0.43 million among people who were HIV-positive (WHO, 2012). This is a slight reduction from the reported figures of new cases of TB in 2009 (WHO, 2010a) but the impact of HIV infection on mortality is still on the increase (WHO, 2012) and is one of the top killers of women, with 300,000 deaths among HIV-negative women and 200,000 deaths among HIV-positive women in 2011. This is despite the availability of treatment that will cure most cases of TB. Short-course regimens of first-line drugs that can cure around 90% of cases have been available since the 1980s (WHO, 2003; ATS, 2003).

While efforts are being made on the progress towards global targets for reductions in TB cases and deaths (Raviglione, 2006; WHO, 2003, 2012), with a mortality rate decreased by 36% since 1990 and the world appears to be on track to achieving the global target of a 50% reduction by 2015, the global burden of TB remains enormous, being highest in Asia and Africa 59 and 26%, respectively (WHO, 2012). Almost 80% of TB cases among people living with HIV reside in Africa. TB incidence rates in Africa are among the highest in the world (Raviglione et al., 1995; Dye et al., 1999, WHO, 2009, 2010a) and these rates have increased steadily over the past two decades as a result of the HIV epidemic (Cantwell and Binkin, 1996; Raviglione, 2006), the strongest known risk factor for the progression from tuberculosis infection to disease (Rieder, 1999), increasing susceptibility to primary tuberculosis and reactivation of latent tuberculous infection, thus increasing tuberculosis incidence directly (Harries, 1990; Perriens et al., 1991; De Cock et al., 1992; Range et al., 2001; WHO 2012).

Worldwide, 3.7% of new cases and 20% of previously treated cases were estimated to have multi-drug resistant tuberculosis (MDR-TB) (WHO, 2012; Connell et al., 2011). India, China, the Russian Federation and South Africa have almost 60% of the world's cases of MDR-TB. The highest proportions of TB patients with MDR-TB are in Eastern Europe and central Asia (WHO, 2012).

Current treatment of TB is usually the combination of isoniazid (INH) and rifampicin, which are given for at least six months, along with pyrazinamide and ethambutol (or streptomycin), which are used only in the first two months (WHO, 2003, 2010b, 2012; ATS, 2003). This treatment regime is referred to as short-course chemotherapy (Addington, 1979; Jawetz, 1987; NIAID, 1999; WHO, 2010b) and its success has been demonstrated through the Directly observed treatment short course (DOTs) and "Stop TB Strategy (WHO, 2010a; 2012). Major progress

in global TB control followed the widespread implementation of the DOTS strategy (Raviglione and Uplekar, 2006; WHO, 2003, 2006).

Antituberculous drugs are generally safe but can occasionally be associated with life-threatening complications, since there has been sporadic reports of cases of neurotoxicity following use of the drug in the initiation of antituberculous therapy (Bharat et al., 2003), and as a preventive therapy (Martinjak-Dvorsek et al., 2000). INH is one of the anti-tuberculosis drugs widely prescribed for patients since the early 1950s. It is relatively nontoxic but some patients develop peripheral neuropathy attributed to a disturbance of vitamin B_6 metabolism. The incidence of acute isoniazid (INH)-related poisonings has increased, with parenteral pyridoxine as the antidote for INH-induced seizures (Romero and Kuczler, 1998; Santucci et al., 1999; Citak et al., 2002; Desai and Agarwal, 2004). While some isoniazid metabolites are hepatotoxic, little is known about their neurotoxic property (Sanfeliu et al., 1999; Kass and Shandera, 2010).

This study is an immunohistochemical evaluation of the cerebral cortex for microchemical and structural anomalies that could possibly underlie the adverse effects of chronic administration of combined INH and rifampicin.

MATERIALS AND METHODS

Adult wistar rats (*Rattus norvegicus*) of either sex (average weight 220 g) used for the experiment were maintained under standard laboratory conditions, fed with standard mouse chow (Ladokun Feeds, Ibadan, Nigeria) and provided with water *ad libitum*. All experimental protocols and animal use and care were approved by the University Research and Ethical Committees. The animals were randomly assigned into two groups (n = 10). Group (A) received a combined dose of 50 mg/kg body weight of INH and Rifampicin (Smithkline-Beecham, Nigeria) administered intraperitoneally (i.p.) daily at 1600 h for 15 days while group B received an equal volume of normal saline (i.p.). A pair-fed group (C) (n = 7) was included to control for the stress of chronic i.p. administration, and received food and water *ad libitum*. Feeding patterns and animal body weights of all groups were monitored throughout the experiment. All animals were monitored closely for clinical signs of neurotoxicity (generalized weakness, ataxia and paralysis of the limbs). At the end of administration, animals were sacrificed by cervical dislocation (n = 6) from Groups A and B; and (n = 4) from Group C and the whole brain was quickly removed, dried with Whatman filter paper No. 1 and weighed. The remaining animals were anaesthetized by an overdose of pentothal intraperitoneally, whole-body perfused under gravity, first with normal saline, followed by 10% formol calcium fixative.

The brains were removed and a 6 mm coronal sample of the frontoparietal cortex (para central sulcus) was taken from each hemisphere under stereoscopic dissection and further fixed in the same fixative for 4 h. Specimens of samples were processed routinely for paraffin embedding and 6 µm thick sections cut on a sliding microtome (Histoslide 2000, Hamburg, Germany), mounted unto slides and left overnight at 37°C in the incubator (for good adherence to the frost slides). The remaining samples were cryosectioned (Fibrigol cryocut) at -23°C, after cryoprotection in 30% sucrose/PBS and 30 µm thick sections were then cut, stored in wells containing 1 ml of acidic phosphate buffered saline (PBS)

at 2 to 8°C before immunohistochemistry.

NISSL staining

Slides of paraffin sections were dewaxed and rehydrated according to standard protocol and stained in 2% cresyl violet solution (Nissl stain) for 5 to 10 min, rinsed briefly in distilled water and then dehydrated with ascending grades of alcohol, cleared in xylene and mounted using Canada balsam and cover slipped.

GFAP immunohistochemistry

Sections were washed thrice for 5 min in tris buffered saline (TBS) (pH 7.4), then blocked in 2% bovine serum with 5% normal goat serum (NGS) for one hour at room temperature. Incubation was done with Cy3-coupled-monoclonal anti-GFAP-antibody [Sigma (1:500)] in blocking solution for 2 h at room temperature. Sections were again washed thrice for 5 min in TBS (pH 7.4) and mounted on gelatinized slides and air dried overnight.

Tunel reaction

Apoptosis of nuclei were assessed by *in situ* terminal deoxynucleotidyl transferase (TdT)-mediated deoxyuridine triphosphate (dUTP)-biotin nick-end labeling (TUNEL) of DNA strand breaks using the *in situ* cell death detection, POD kit, for immunohistochemical detection of apoptosis (Roche Diagnostics, Mannheim, Germany). Sections were transferred unto slides through 0.2 M PBS, pH 7.4, and allowed to air-dry overnight. The following day, they were washed in PBS for 30 min. To block endogenous peroxidase activity and improve cell permeability, sections were rinsed with PBS and incubated with blocking solution (3% H_2O_2 in methanol) for 10 min at room temperature, then rinsed in PBS and incubated in permeabilisation solution for 2 min on ice (4°C). Labeling was done by rinsing sections in PBS twice, the area around the section dried with filter paper and 50 µl TUNEL reaction mixture was added onto the section, cover slip applied (to avoid evaporative loss and ensure homogenous spread of the mixture) and then incubated in a humidified chamber for 60 min at 37°C. For positive control, sections of rat ileum were incubated simultaneously without the enzyme in the reaction mixture. Sections were rinsed with PBS thrice. The areas around sections were dried again for signal conversion and analysis. 50 µl of converter-POD was added onto the section, cover slip applied (to avoid evaporative loss and ensure homogenous spread of the mixture) and then incubated in a humidified chamber for 30 min at 37°C, then rinsed thrice with PBS. A 50 to 100 µl sigma-3,3'-diaminobenzidine (DAB) substrate solution was added to sections and incubated for 10 min at room temperature, rinsed thrice with PBS and counter stained in nissl stain, dehydrated, cleared and mounted in entellan.

Image analysis

Sections were examined using Axioplan-2 epiflourescence photomicroscope (Carl Zeiss, Germany), with a Sony 3-CCD video camera (Tokyo, Japan) connected to a Compaq computer that has the AxioVision 3.0-Rel. software for digital image analysis. Images were opened in Adobe Photoshop (version 6; Adobe Systems, San Jose, CA) and stored in a TIFF file format on the hard drive. Photomicrographs were produced from the grabbed frames and printed on Hp premium photo glossy paper using an Hp 5700 DeskJet printer.

Quantification of immunocytochemical staining

For the entire study, the camera had its auto mode turned off and manual controls were used to adjust the image intensity which was kept at an identical level during the entire study. All images obtained from treatment and control groups were at the same level of magnification. Five fields were chosen so as to best reflect the overall immunostaining of the reactivity on the entire slide. The digitized images were stored on an external data storage device (IOGEAR 2.5" eSATA 3Gbps/USB 2.0 Combo ION™ External Hard Drive) until required.

The procedure for determination of immunostaining intensity and the technique of selection of similar features on a digitized immunohistochemical image has previously been described in detail (Lehr et al., 1996, 1997, 1999). The software used in this study was Adobe Photoshop Elements, version 6.0 (20070910.r.377499). Briefly, using the magic wand tool in the tool menu of Photoshop Elements 6.0, the cursor was placed on a GFAP-positive astrocyte. The tolerance level of the magic wand tool was adjusted so that the entire astrocyte was selected. Using the similar command in the select menu, all immunostained astrocytes were automatically selected. Subsequently, the image was transformed to 8-bit grayscale. An optical density plot of the selected area was generated using the histogram tool in the window menu. The mean staining intensity (in arbitrary units, AU) was recorded. Following this, the background was selected using the inverse tool in the select menu, and immunostaining was quantified using the histogram tool in the window menu. Immunostaining intensity was calculated as the difference between astrocytic immunostaining and background immunostaining and was designated as immunocytochemical index with arbitrary units (AU). The quantification of immunostaining data is presented in Figure 4.

Statistical analysis

The data were analyzed using the computerized statistical package 'Statistica 5.0'. The mean and standard error of mean (SEM) values for each group was determined. The means were compared by analysis of variance at a level of significance of 95 and 99%. However, the immunocytochemical index is unitless and hence values are therefore reported as energy units per pixel (eu/pix). In all instances, data are expressed as the means ± SEM.

RESULTS

Administration of combined INH/rifampicin did not affect the appetite of the animals and no clinical signs of neurotoxicity were observed, while there was no significant difference in the mean absolute and relative brain weights of the treatment group compared to the control (p > 0.05). Values were mean + SEM (Figure 1). The results showed no significant changes on the body weights of the animals throughout the duration of the experiment.

Combined INH and rifampicin induced highly reactive intracortical GFAP positive astrocytes, localized in clusters in the cerebral cortex (Figure 2a and c), while the control animals showed uniform distribution of GFAP signals across the cortex (Figure 2b and d). Astrocytes were intensely and brilliantly florescent, robust with short and heavy branching limbs (Figure 2c) compared to the slender, long and fewer branches seen in the control group (Figure 2d). The pial and subpial regions demonstrated GFAP positive reactions in both treatment (Figure 3a and b) and control groups (Figure 3c and d),
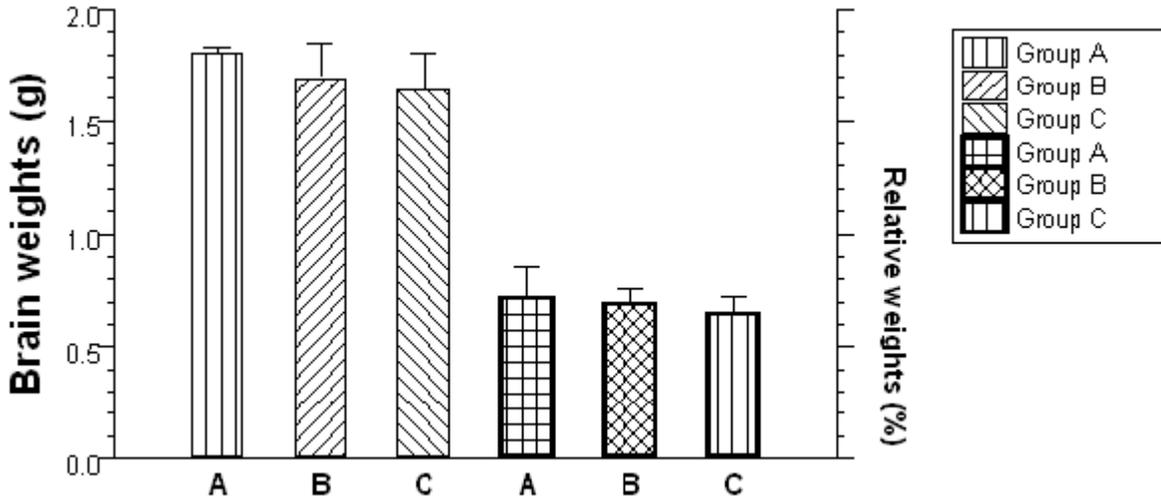
Figure 1. Mean absolute and relative brain weights of rats administered combined INH/rifampicin. Values are mean ± SEM ($p > 0.5$) [A and B: (n = 6); C: (n = 4)].
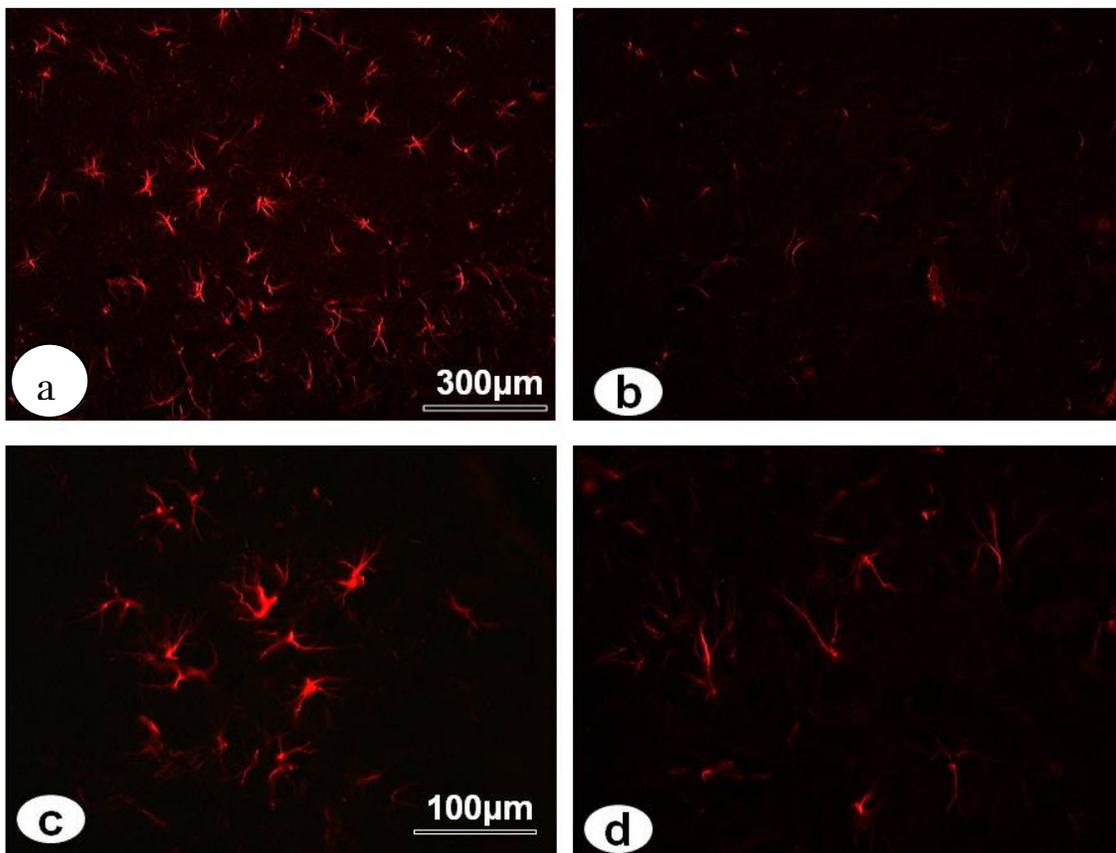
Figure 2. GFAP Immunohistochemistry of the cerebral cortex showing reactive astrocytosis in the treatment group (a, c) compared to control group (b, d). Bars: [a, b - 300 µm; c, d – 100 µm].

with the treatment group being slightly more reactive than the control group. The quantification of immunostaining intensity of GFAP immunoreactivity revealed significantly higher intensity over the entire cerebral cortex in the
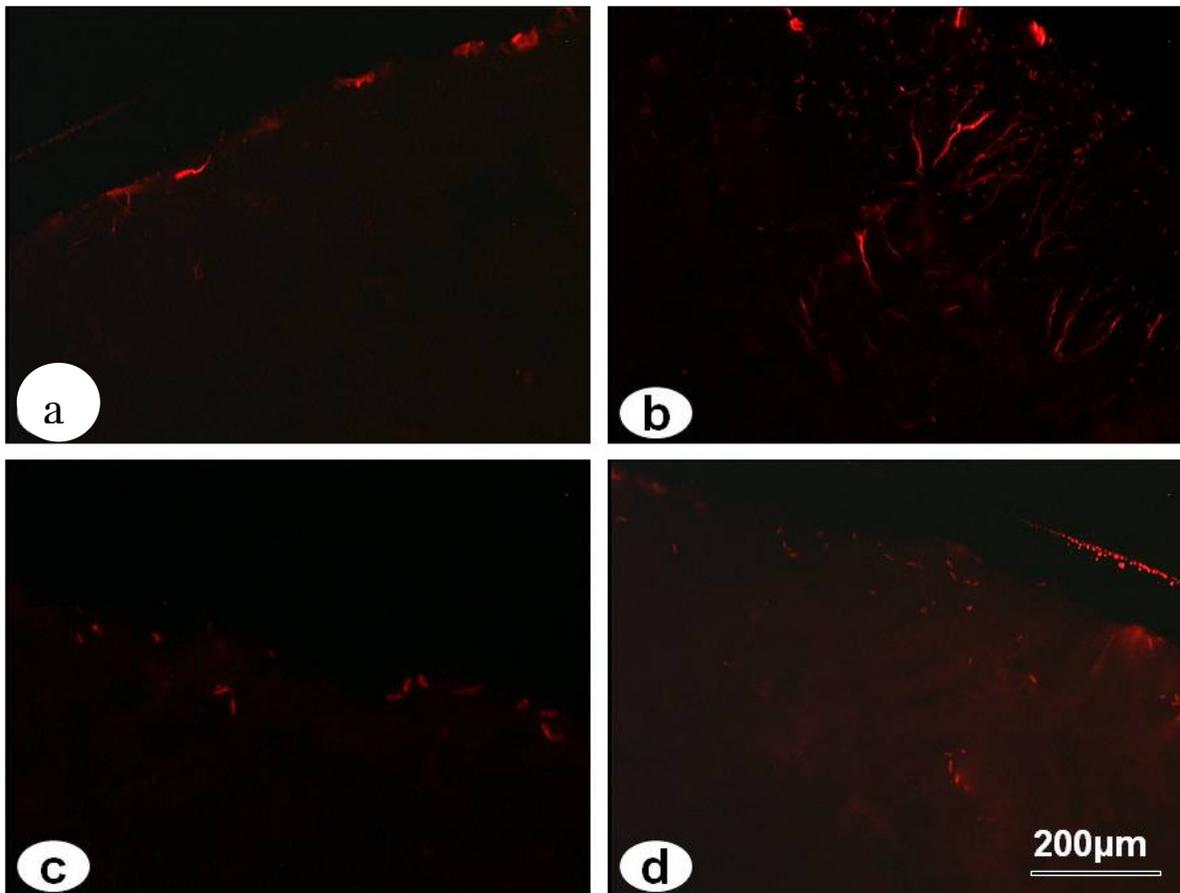
Figure 3. GFAP Immunohistochemistry of pial and subpial regions of the cerebral cortex showing significant immunostaining in the treatment group (a, b) compared to control group (c, d), respectively. Bar: 200 µm.

treatment group compared to the controls, even though slightly less in the pial region (Figure 4)

Nissl staining revealed an even distribution of the cortical lamina layers in all groups (Figure 5a and b). There were close apposition of densely stained 'peanut-shaped' bodies to neurons in the treatment group (Figure 5c) in contrast to the control (Figure 5d). Most of these bodies appear granulated. Neither cortical lamina distortion nor neuronal pyknotism were observed in the groups (Figure 5a and b).

TUNEL reaction revealed numerous intensely stained dark-brown cells of varying sizes, generalized over the cortex (Figure 6a) in the treatment group. No predilection for particular lamina in the treatment group. The control group showed few slightly stained cells positive for the TUNEL reaction (Figure 6b). The positive control was negative for the reaction.

DISCUSSION

The first line drugs in the treatment of TB remains isoniazid, rifampicin and ethambutol in Africa, Asia and parts of Latin America, where TB as a chronic inflammatory condition is still very prevalent, with increase in incidence due to the human immune deficiency virus/acquired immune deficiency syndrome (HIV/AIDs) scourge (WHO, 2012). Since the organism (*Mycobacterium tuberculosis*) (been intracellular and exhibiting long periods of metabolic inactivity) tends to develop resistance to any one drug, the combination drug treatment is employed (Addington, 1979; Dutt and Stead, 1982; Jawetz, 1987). The results of this study showed no clinical signs of neurotoxicity or changes in body weight or feeding pattern following chronic administration of combined isoniazid and rifampicin. Absolute and relative brain weight differences were not statistically significant.

Pyridine-4-carboxy hydrazide (isonicotinyl hydrazide; isoniazid - INH), the hydrazide of isonicotinic acid, (MW 137) is a simple molecule freely soluble in water, that has been used in the treatment of TB for over six decades, while rifampicin was introduced in 1963 (Connell et al., 2011). Neurotoxic effects of INH were reported since the early 1950s, with complications of peripheral neuritis,
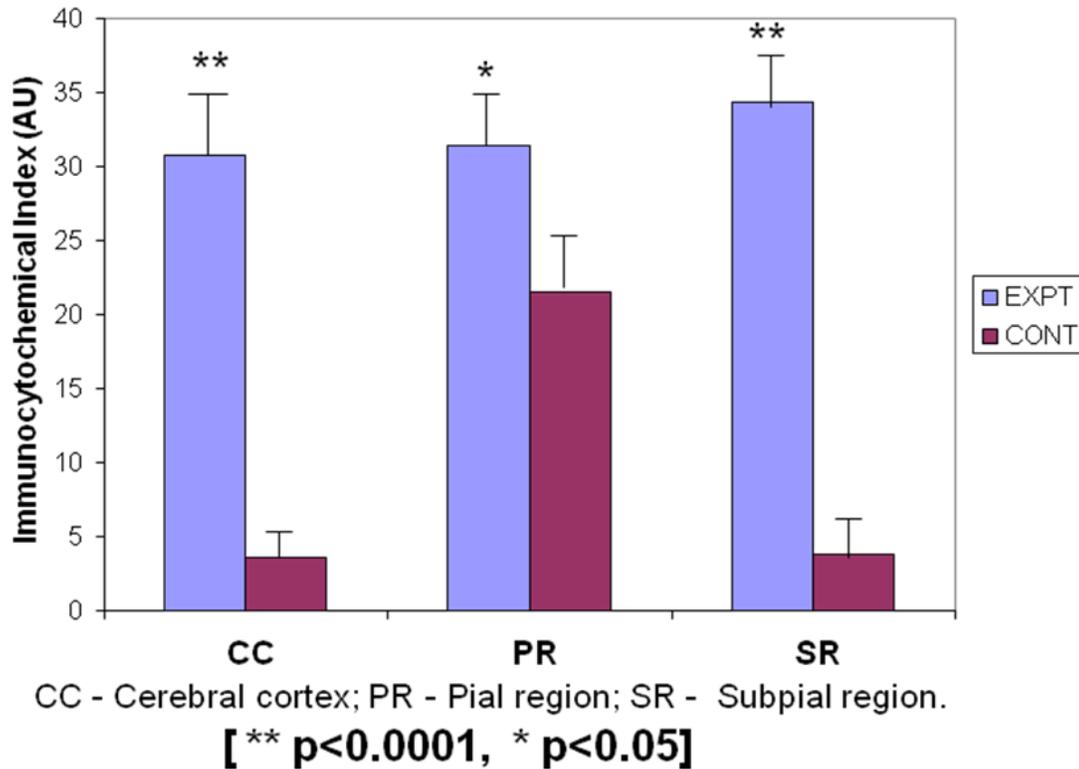
Figure 4. Quantification of GFAP immunoreactivity in the cerebral cortex (CC), pial region (PR) and subpial regions (SR) of the treatment and control groups compared.

convulsions, optic atrophy with blindness, and major psychoses being major features in up to 5% of patients (BMJ, 1958). Similar neurotoxic features have also been reported in animal studies (BMJ, 1958). Acute isoniazid intoxication is characterized by symptoms of vomiting, rapid onset of seizures, with or without fever particularly in children (Shah et al., 1995), metabolic acidosis (Koster et al., 1985) and prolonged obtundation (Citak et al., 2002). Isoniazid is also reported to be toxic to the optic nerve (Thomas, 1994; Desai and Agarwal, 2004), creating a mild sensory polyneuropathy and a bilateral retrobulbar neuritis which can progress to a severe optic atrophy (Leppert and Waespe, 1988) and acute cerebellar dysfunction (Blumberg and Gil, 1990). These complications have been attributed to a relative pyridoxine deficiency which can be prevented by administration of pyridoxine (Byrd et al., 1979; Lewin, 1996; Citak et al., 2002).

Our study showed that combined INH/rifampcin administration for 15 days in adult wistar rats produced astrocytic aggregation and hyperactivity in the cerebral cortex. Astrocytes are major neuronal supports that react to brain assault by aggregating, becoming enlarged in what is referred to as astrogliosis or so-called "reactive gliosis," a reaction with specific structural and functional characteristics (Pekny and Nilsson, 2005; Raivich et al.,

1999; McGraw et al., 2001; Tacconi, 1998; Hatten et al., 1991). The marked immunostaining intensity of reactive astrogliosis was quantified using the Adobe Photoshop Element 6.0 as previously described by Lehr et al. (1996, 1997). This technique was found to be highly dis-criminatory and easy to establish. Once the chromogen is selected, quantification is accomplished using the histogram command in the window menu. The histogram is used to analyze the image's tonal distribution which is shown as the distribution of an image's pixel values in a bar chart. The information derivable from the histogram display include mean (represents the average intensity value), standard deviation (SD) (represents how widely intensity values vary), median (shows the middle value in the range of intensity values), pixels (represents the total number of pixels used to calculate the histogram) (Adobe Help resource Center). The slight elevation of glial fibrillary acidic protein expression in astrocytes of superficial glial limiting membrane in the treatment group usually is a response to sustained injury, which is supported by the presence of large number of apoptotic processes taking place in the cortex. A double labeling for TUNEL reaction and GFAP reactivity would precisely confirm whether astrocytes were also undergoing apoptosis.

Sanfeliu et al. (1999) showed that in cultures studies
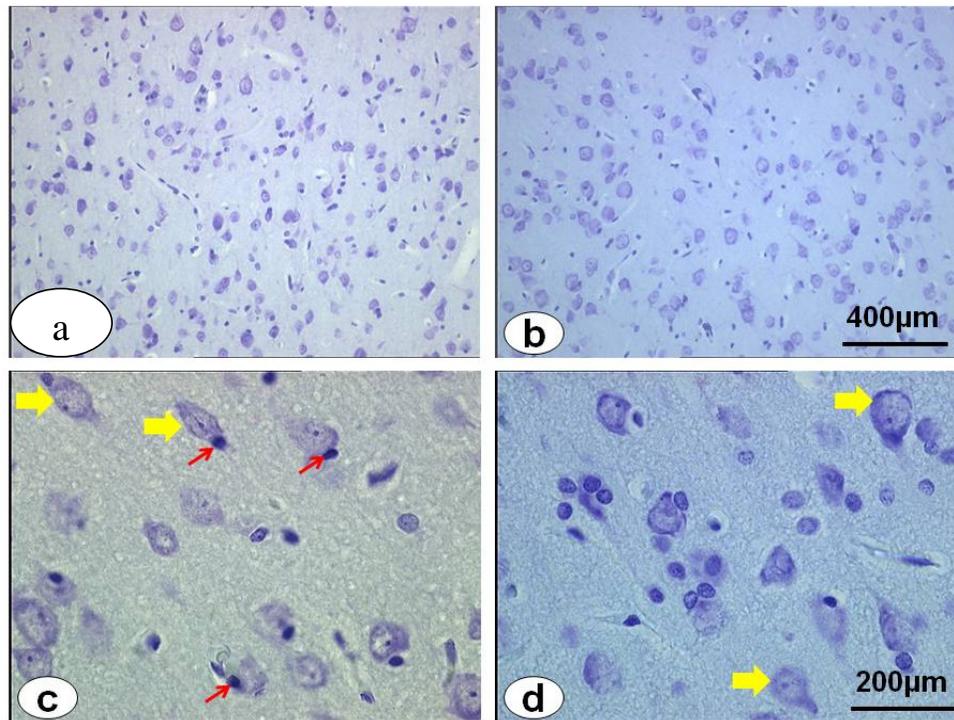
Figure 5. Effects of Combined INH/rifampicin administration on the cerebral cortex of the treatment group (a, c) compared to control (b, d) Nissl stain; [Red arrows – "peanut bodies"; yellow arrows – pyramidal neurons]. Bars: [a, b – 400 μm; c, d – 200 μm].

of mouse dorsal root ganglion (DRG) neurons and N18D3 mouse hybrid neurons, isoniazid did not cause neurotoxicity at exposures up to 7 days and hydrazine was found to be the most toxic metabolite with LC_{50} values of 2.7 and 0.3 mM after 7 days of exposure to DRG neurons and N18D3 hybrid neurons, respectively. This is supported by our findings of microstructural and microchemical anomalies after 15 days of administration of INH/rifampicin. Since 1952, when the drug was first introduced, multiple INH metabolites have been identified, including hydrazine (HZ), isonicotinic acid (INA), ammonia, the acetylated derivative N(1)-acetyl-N(2)-isonicotinylhydrazide (AcINH), hydrazones with pyruvic and ketoglutaric acids (INH-PA and INH-KA, respectively), monoacetylhydrazine (AcHZ), diacetylhydrazine (DiAcHZ), and oxidizing free radicals (Preziosi, 2007). Their formation is the result of hydrolysis (INA, HZ), cytochrome P450 (CYP)-dependent oxidation (HZ, NH(3), oxidizing free radicals), and N-acetyltransferase (NAT) activity (AcINH, AcHZ, DiAcHZ).

Doubts remain about isonicotinamide (INAAM) as an INH metabolite in mammals (Preziosi, 2007). Sanfeliu et al. (1999) suggested that metabolites including acetylisoniazid, acetylhydrazine, diacetylhydrazine and isonicotinic acid had moderate to minor neurotoxic effects on N18D3 hybrid neurons. However, pyridoxine, which is used in clinical practice to prevent or ameliorate the

isoniazid-induced neuropathy (Santucci et al., 1999; Citak et al., 2002), did not consistently reverse the neurotoxicity of any of the metabolites in the cell cultures. Pyridoxine itself was found to be neurotoxic both in DRG neurons and N18D3 hybrid neurons, in agreement with human peripheral sensory neuropathy caused by prolonged overdosage (Sanfeliu et al., 1999). Pyridoxine (vitamin B6) is a co-factor in many enzymatic pathways involved in amino acid metabolism; the main biologically active form is pyridoxal 5-phosphate (Lheureux et al., 2005). The enzymes catalase and superoxide dismutase and the antioxidant agent selenium were reported to show some protection against hydrazine neurotoxicity, suggesting an involvement of the generation of reactive oxygen species in the pathogenesis of isoniazid neuropathy.

Astrogliosis, characterized by the enhanced expression of GFAP, represents a remarkably homotypic response of astrocytes to all types of injuries of the central nervous system (CNS), including injuries to the developing CNS. As such, astrocytes serve as microsensors of the injured microenvironment regardless of their location in the CNS. The diversity of insults that engender astrogliosis and the brain-wide nature of the astrocytic response suggest that common injury factors serve as the trigger of this cellular reaction. Reactive gliosis traditionally has been examined qualitatively by immunohistochemistry of GFAP (O'Callaghan, 1994), and the prominent theme that has
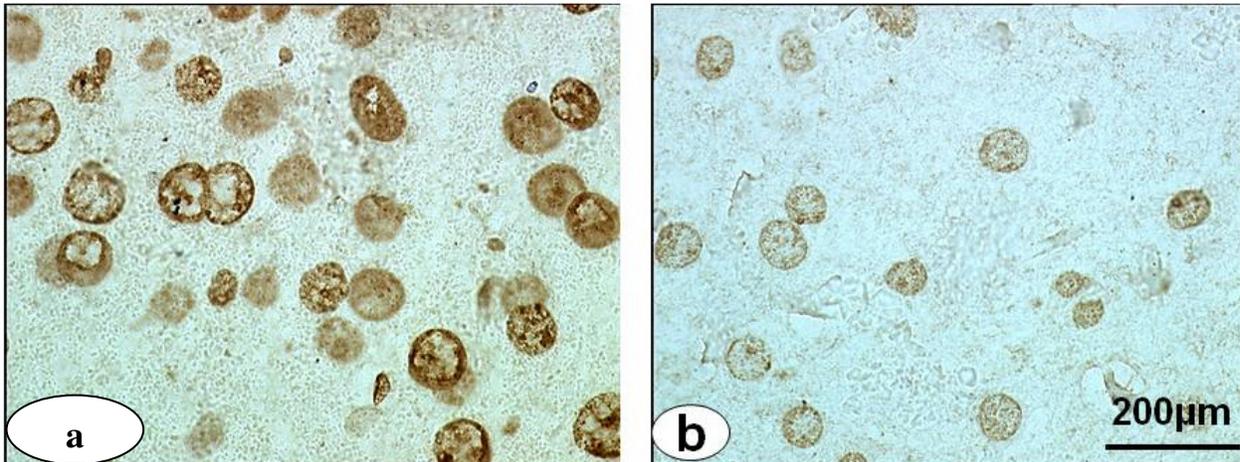
Figure 6. Effects of combined INH/rifampicin administration on the cerebral cortex of the treatment group (a) and control group (b) TUNEL reaction. Bar: 200 μm.

emerged in recent years is that proinflammatory cytokines and chemokines serve as a stimulus for induction of astrogliosis (Little and O'Callagha, 2001).

The numerous TUNEL positive cells are a strong indication of an active programmed cell death induced by the combined drug administration in the treatment group. With no particular predilection for any cortical lamina, it was unlikely however that all the apoptotic cells were neurons only. A double labeling for TUNEL reaction and GFAP reactivity would precisely confirm the involvement of astrocytes undergoing apoptosis. The cortical lamina was well preserved in all groups. The presence of few stained TUNEL positive cells in the control groups is an indication of lack of foolproof of the method. Apoptosis has been observed in a myriad of physiological and pathophysiological conditions (Kerr et al., 1972; Hengartner, 1998; Barinaga, 1998) including normal development, morphogenesis, disease conditions and degenerative disorders. However, Gal et al. (2000) has demonstrated TUNEL positivity of non-apoptotic fixed cells elicited by proteases, and was detected in both formaldehyde- and ethanol-fixed specimens in agarose-embedded fixed cells, and in chromatin spreads.

By urea-agarose gel electrophoresis, the average single-strand size of the DNA molecules carrying the free ends was found between 50 and 250 kb. They suggested that s=s discontinuities preexisting in the fixed normal cells are unmasked by protease treatment eliciting TUNEL positivity (Gal et al., 2000). While this study confirms that chronic administration of combined INH/rifampicin induces microchemical neurotoxicity in the cerebral cortex of wistar rats, how this plays out clinically is not yet known. There is a need to examine these agents in animal models of the disease and for longer periods to determine the manifestations of these microchemical changes observed within just two weeks of administration. When these agents are used for long periods in the treatment of TB, it is imperative that users are monitored closely for any manifestation, even after the medications has been discontinued.

Although most physicians are aware of INH hepatotoxicity, acute INH poisoning and its treatment are not well recognized. INH is increasingly being used to control the spread of tuberculosis, and health providers should be aware and alert with heightened suspicious index for its potential toxic effects. Given the prolonged and occasionally arduous nature of anti-tuberculous treatment for patients, we face an increasing incidence of multi-drug-resistant tuberculosis (MDR-TB), defined as infection with *M. tuberculosis* that is resistant to both rifampicin and isoniazid. Resistance to multiple anti-tuberculous drugs has arisen for a number of reasons; however, it can be argued that the principle reasons for these are the indiscriminate or poorly managed use of antibiotics, coupled with a lack of drug susceptibility testing in regions where it is most needed (Conde et al., 2009; Hall et al., 2009).

There is therefore a challenge not only to find new drugs to treat increasingly drug-resistant TB but also to find drugs that will allow shorter treatment courses and less complication. Second-line agents are used in cases of intolerance or some other contraindication to the firstline antituberculosis agents (rifampin, isoniazid, pyrazinamide, and ethambutol) and consist of cycloserine, ethionamide, *p*- minosalicylic acid (PAS), capreomycin, and the aminoglycosides. Fluoroquinolones are recommended as second-line agents but are being tested in multicenter trials as first-line agents (Hall et al., 2009). Several clinical trials are testing the possibility of replacing isoniazid with moxifloxacin, in an attempt to reduce duration of therapy to 4 months (Hall et al., 2009; Connell et al., 2011).

With an average of about 3.2 million new TB cases, Africa accounts for a quarter of the global total, and has

the highest incidence and prevalence rates of any region (WHO, 2010a, 2012). Thirteen of the 15 countries with the highest incidence rates in the world, and 9 of the 22 high burden countries (HBCs), are in Africa (WHO, 2012). Hence, it is important to evaluate the impact of these drugs on different parts of the brain to determine how it will affect users on the long term.

ACKNOWLEDGEMENTS

REFERENCES

Addington WW (1979). Treatment of pulmonary tuberculosis: Current options. Arch Intern Med 139:1391.
Adobe Help Resource center: http://help.adobe.com/en_US/PhotoshopElements/6.0/. Accessed on May 15th 2009.
ATS, American Thoracic Society (2003). Centers for Disease Control and Prevention, Infectious Diseases Society of America. Treatment of tuberculosis. MMWR Recomm. Rep 52:1–77. (Erratum in MMWR Recomm. Re. 53:1203.
Barinaga M (1998). Death by dozens of cuts. Science 280:32-34.
Bharat A, Vedkumar M, Subhash HS, Abraham OC, Mathai D (2003) Antituberculous therapy-induced toxicity. J Assoc. Physicians India 51:522-524
Blumberg EA, Gil RA (1990). Cerebellar syndrome caused by isoniazid. DICP 24:829-831
BMJ (1958) Neurotoxic Effects of Isoniazid. Br. Med. J. 1(5075):880-881.
Byrd RB, Horn BR, Solomon DA, Griggs GA (1979) Toxic effects of isoniazid in tuberculosis chemoprophylaxis. Role of biochemical monitoring in 1,000 patients. JAMA 241:1239-1241
Cantwell MF, Binkin NJ (1996). Tuberculosis in sub-Saharan Africa: a regional assessment of the impact of the human immuno-412 deficiency virus and National Tuberculosis Control Program quality. Tuberc. Lung Dis. 77: 220–225
Citak A, Kaya O, Ucsel R, Karabocuoglu M, Uzel N (2002). Acute isoniazid neurotoxicity in childhood. Turk. J. Pediatr. 44:54-57
Conde MB, Efron A, Loredo C, De Souza GR, Graça NP, Cezar MC, Ram M, Chaudhary MA, Bishai WR, Kritski AL, Chaisson RE (2009). Moxifloxacin versus ethambutol in the initial treatment of tuberculosis: a doubleblind, randomised, controlled phase II trial. Lancet 373:1183–1189
Connell DW, Berry M, Cooke G, Kon OM (2011) Update on tuberculosis: TB in the early 21st century. Eur. Respir. Rev. 20:71–84
De Cock KM, Soro B, Coulibaly IM, Lucas SB (1992). Tuberculosis and HIV infection in Sub-Saharan Africa. JAMA 268:1581–1587
Desai VA, Agarwal SB (2004). Isoniazid Toxicity. J. Indian Acad. Clin. Med. 5:83-5
Dutt AK, Stead WW (1982). Present chemotherapy for tuberculosis. J. Infect. Dis. 146:698
Dye C, Scheele S, Dolin P, Pathania V, Raviglione MC, WHO Global Surveillance and Monitoring Project (1999). Global burden of tuberculosis: estimated incidence, prevalence, and mortality by country. JAMA 282:677–686
Gál I, Varga T, Szilágyi I, Balázs M, Schlammadinger J, Szabó G, Jr (2000). Protease-elicited TUNEL Positivity of Non-apoptotic Fixed Cells. J. Histochem. Cytochem. 48:963–969.
Hall RG, Leff RD, Gumbo T (2009). Treatment of Active Pulmonary Tuberculosis in Adults: Current Standards and Recent Advances. Pharmacotherapy 29:1468–1481.

Harries AD (1990) Tuberculosis and human immunodeficiency virus infection in developing countries. Lancet 335: 387–390
Hatten ME, Liem RK, Shelanski ML, Mason CA (1991). Astroglia in CNS injury. Glia 4:233-43.
Hengartner M (1998). Apoptosis. Death by crowd control. Science 281:1298-1299.
Jawetz E (1987). Antimycobacterial drugs. In: Katzung BG (ed.), Basic and Clinical Pharmacology. Appleton and Lange, California. pp. 135-139.
Kass JS, Shandera WX (2010). Nervous system effects of antituberculosis therapy. CNS Drugs 24:655-67.
Kerr JF, Wyllie AH, Currie AR (1972) Apoptosis: a basic biological phenomenon with wide-ranging implications in tissue kinetics. Br. J. Cancer 26:239-257.
Koster B, Bode U, Weber HP, Musch E (1985). Acute isoniazid poisoning. Anasth. Intensivther Notfallmed 20:32-4.
Lehr HA, Hansen KD, Coltrera MD, Russ JC, Gown AM (1996). Photoshop-based image analysis for the semiautomated assessment of Ki-67-defined proliferative activity in the routine diagnosis of breast cancer. Appl. Immunohistochem 4:117-121.
Lehr HA, Mankoff DA, Corwin D, Santeursanio G, Gown AM (1997). Application of Photoshop-based image analysis to quantification of hormone receptor expression in breast cancer. J. Histochem. Cytochem. 45:1559-1565.
Lehr HA, van der Loos CM, Teeling P, Gown AM (1999). Complete chromogen separation and analysis in double immunohistochemical stains using Photoshop-based image analysis. J. Histochem. Cytochem. 47:119-125.
Leppert D, Waespe W (1988) Neurotoxicity of antituberculous drugs in a patient without active tuberculosis. Ital. J. Neurol. Sci. 9:31-34.
Lewin PK. (1996) Isoniazid Neurotoxicity. Pediatrics 5:782-783.
Lheureux P, Penaloza A, Gris M (2005). Pyridoxine in clinical toxicology: a review. Eur. J. Emerg. Med. 12:78-85.
Little AR, O'Callagha JP (2001) Astrogliosis in the adult and developing CNS: is there a role for proinflammatory cytokines? Neurotoxicology 22:607-18.
Martinjak-Dvorsek I, Gorjup V, Horvat M, Noc M (2000) Acute isoniazid neurotoxicity during preventive therapy. Crit Care Med. 28:567-568
McGraw J, Hiebert GW, Steeves JD (2001). Modulating astrogliosis after neurotrauma. J. Neurosci. Res. 63:109-115.
O'Callaghan JP (1994). Biochemical analysis of glial fibrillary acidic protein as a quantitative approach to neurotoxicity assessment: advantages, disadvantages and application to the assessment of NMDA receptor antagonist-induced neurotoxicity. Psychopharmacol. Bull. 30:549-554.
Pekny M, Nilsson M (2005). Astrocyte activation and reactive gliosis. Glia 4:427-434.
Perriens JH, Mukadi Y, Nunn P (1991). Tuberculosis and HIV infection: implications for Africa. AIDS 43:127–133.
Preziosi P (2007). Isoniazid: metabolic aspects and toxicological correlates. Curr. Drug Metab. 8:839-51.
Raivich G, Jones LL, Werner A, Bluthmann H, Doetschmann T, Kreutzberg GW (1999). Molecular signals for glial activation: pro- and anti-inflammatory cytokines in the injured brain. Acta Neurochir Suppl. 73:21-30.
Range N, Ipuge YA, O'Brien RJ, Egwaga SM, Mfinanga SG, Chonde TM, Mukadi YD, Borgdorff MW (2001). Trend in HIV prevalence among tuberculosis patients in Tanzania, 1991-1998. Int. J. Tuberc. Lung Dis. 5:405-412.
Raviglione MC (2006). The Global Plan to Stop TB, 2006–2015. Int. J. Tuberc. Lung Dis 10: 238–239.
Raviglione MC, Snider DE, Kochi A (1995) Global epidemiology of tuberculosis. Morbidity and mortality of a worldwide epidemic. JAMA 273:220–226.
Raviglione MC, Uplekar MW (2006) WHO's new stop TB strategy. Lancet 367:952–955.
Rieder H L (1999). Epidemiologic basis of tuberculosis control. International Union Against Tuberculosis and Lung Disease, Paris.
Romero JA, Kuczler FJ (1998). Isoniazid overdose: recognition and management. Am. Fam. Physician 57:749-752.
Sanfeliu C, Wright JM, Kim SU (1999). Neurotoxicity of isoniazid and its metabolites in cultures of mouse dorsal root ganglion neurons and

hybrid neuronal cell line. Neurotoxicology 20:935-44.

Santucci KA, Shah BR, Linakis JG (1999). Acute isoniazid exposures and antidote availability. Pediatr. Emerg. Care 15:99-101.

Shah BR, Santucci K, Sinert R, Steiner P (1995). Acute isoniazid neurotoxicity in an urban hospital. Pediatrics 95:700-4.

Tacconi MT (1998) Neuronal death: is there a role for astrocytes? Neurochem. Res. 23:759-65

Thomas RJ (1994). Neurotoxicity of antibacterial therapy. South Med. J. 87:869-74

WHO, World Health Organisation (2003). Treatment of tuberculosis: guidelines for national programmes, 3rd ed. World Health Organization (WHO/CDS/TB/2003.313), Geneva.

WHO (2006). The global plan to stop TB, 2006–2015. World Health Organization, Geneva. (WHO/HTM/STB/2006.35).

WHO, World Health Organisation (2009). Global Tuberculosis Control 2009 – Epidemiology, Strategy, Financing. Global Tuberculosis Control 2009 – A Short Update to the 2009 report; World Health Organization, Geneva.

WHO, World Health Organisation (2010a). Report Global Tuberculosis Control (2010) Fifteen annual report. World Health Organization, Geneva.

WHO, World Health Organisation (2010b). Treatment of tuberculosis: Guidelines – 4th ed. Geneva, World Health Organization, 2010 WHO/HTM/TB/2009.420.

WHO, World Health Organisation (2012). Global tuberculosis report 2012. Geneva, World Health Organization. WHO/HTM/TB/2012.6.